Autonomous division of the outer membrane in Gram-negative bacteria

Carolina Basurto De Santiago and Beiyan Nan*

Department of Biology, Texas A&M University, College Station, Texas, USA

*Correspondence: Beiyan Nan, bnan@tamu.edu

Abstract

Gram-negative bacteria divide by separating two cell wall layers: peptidoglycan (PG) and the outer membrane (OM). In certain model organisms, the OM is tethered to PG, ensuring it closely follows PG throughout invagination, constriction, and separation. In contrast, *Myxococcus xanthus* exhibits autonomous OM partitioning, occurring only after complete PG fission. However, reinforcing the OM-PG connection by overexpressing endogenous or exogenous tethering proteins synchronizes the constriction and fission of both layers.

14 The cell wall of Gram-negative bacteria consists of two distinct layers: a
15 peptidoglycan (PG) meshwork and an outer membrane (OM). PG is a single
16 macromolecule of glycan strands crosslinked by short peptides. The OM is an asymmetric
17 bilayer with lipopolysaccharides (LPS) in the outer leaflet and phospholipids in the inner
18 leaflet [1]. While PG plays a major role in maintaining cell integrity and morphology, the
19 OM serves as a selective barrier that protects the cell from harmful substances, including
20 antibiotics [2,3]. In certain bacteria, such as *Escherichia coli*, OMs are load-bearing structures
21 that can exhibit even greater stiffness than PG [4].

22 During cell division, bacteria constrict and divide PG using a well-organized PG
23 remodeling machinery called the divisome [5]. In contrast, the OMs in Gram-negative
24 bacteria are devoid of energy sources and consequently lack their own dedicated division
25 machinery. To divide the OM, some Gram-negative bacteria tether their OMs to PG. For
26 instance, *E. coli* employs multiple PG tethering systems for the OM. First, the OM contains
27 abundant Braun's lipoprotein (Lpp) that attaches to PG directly through covalent bonds
28 [6]. Second, the OM lipoprotein LpoA and LpoB directly interact with PG synthases to
29 coordinate the growth and division of these two cell wall layers [7-10]. Third, the PG-
30 associated lipoprotein (Pal) attaches to PG noncovalently and connects to the OM
31 components in the Tol-Pal system [11]. Fourth, some β-barrel OM proteins (OMPs) interact
32 with PG noncovalently through their C-terminal OmpA-like domains [12]. Through these
33 tethering mechanisms, the OM closely follows the invagination, constriction, and

34 separation of PG throughout *E. coli* cell division [8,13]. However, Lpp and LpoA/B are only
35 conserved in γ-proteobacteria [9]. It is unclear if the coordinated constriction of PG and OM
36 is a universal division mechanism among Gram-negative bacteria and if the connection
37 between OM and divisome is essential for OM division.

38 To answer these questions, we investigated cell division in *Myxococcus xanthus*, a
39 rod-shaped Gram-negative bacterium. Lacking Lpp and LpoA/B homologs [14], *M. xanthus*
40 may exemplify a wide group of Gram-negative bacteria that lack rigid connections
41 between the OM and PG. Accordingly, in contrast to the rigid *E. coli* OM, the *M. xanthus*
42 OM appears highly fluid, enabling the rapid diffusion of OM proteins, frequent shedding
43 of OM, and active intercellular exchange of OM contents among closely related strains [15-
44 17]. Using *in situ* cryogenic electron microscopy (cryoEM), we captured the micrographs of
45 dividing *M. xanthus* cells, in which the electron densities of the inner membrane (IM) and
46 OM were easily distinguished from the background (**Fig. 1A**). In contrast, the thin PG
47 layer was extremely difficult to visualize (**Fig. 1A**). Since turgor pressure pushes the fluid
48 IM layer against PG, IM closely mirrors the shape of PG during both growth and division.
49 Therefore, we used IM to reflect the constriction and division of PG.

50 In all CryoEM images of dividing wild-type *M. xanthus* cells, the OM exhibited only
51 slight invagination upon complete IM separation, suggesting that PG and OM are
52 uncoupled during division (**Fig. 1A1 - 1A3**). This phenotype is strikingly similar to two
53 *E. coli* filamentous mutants that cannot separate daughter cells: the *ΔenvC ΔnlpD* mutant

54 that cannot hydrolyze septal PG [13] and the *Δlpp Δpal* strain that loses the major
55 connections between PG and OM [18]. However, wild-type *M. xanthus* do not form cell
56 chains, indicating that the uncoupled division of PG and OM does not lead to division
57 defects. To confirm the cryoEM observation, we grew cells in the presence of TAMRA 3-
58 amino-D-alanine (TADA), a red fluorescent D-amino acid that incorporates into PG [19] and
59 stained the OM with Alexa Fluor 488-conjugated wheat germ agglutinin [20]. We selected
60 dividing cells with cytoplasms separated by fewer than 3 pixels (480 nm) in bright-field
61 images and used fluorescence microscopy to visualize a ~200-nm thick longitudinal
62 section containing both PG and OM under highly inclined and laminated optical sheet
63 (HILO) illumination [21-24]. The fluorescence signals of PG at division sites either intensified
64 or vanished entirely, corresponding to the invaginated and separated PG, respectively
65 (**Fig. 1B**). Regardless of the separation of PG, all the dividing cells (n > 100) displayed
66 continuous OM at their division sites (**Fig. 1B**). Crucially, we never detected a surge in
67 OM signal at division sites, confirming that, unlike PG, OM does not undergo gradual
68 invagination in wild-type *M. xanthus* (**Fig. 1B**). Consistent observations from cryoEM and
69 fluorescence microscopy confirmed that, unlike *E. coli*, *M. xanthus* divides its OM
70 autonomously. Based on our recent discovery that the *M. xanthus* OM is highly fluid [15],
71 here we propose a straightforward stretch-and-snap mechanism, where the mechanical
72 stretching of the OM drives its division. However, fluorescence microscopy at up to 67
73 Hz (15 ms/frame) failed to capture such snapping events, suggesting they occurred faster

74 than our detection threshold. Nevertheless, supporting our hypothesis, cryoEM imaging
75 revealed instances of stretched and ruptured OMs between separating daughter cells.
76 (**Fig. 1A2, 1A3**).

77 To investigate how PG-tethering mechanisms affect the mode of OM division, we
78 overexpressed *E. coli* Lpp exogenously in *M. xanthus* and observed synchronized
79 invagination, constriction, and constriction of OM and IM (**Fig. 1A4, 1A5**). Consistently,
80 OM was also synchronized with PG during cell division under fluorescence microscopy
81 (**Fig. 1B**). Notably, we detected a surge in OM signals at certain division sites, suggesting
82 that OM invaginated in a manner similar to PG (**Fig. 1B**). In contrast, the overexpression
83 of a truncated Lpp that lacked the terminal lysine ($Lpp_{\Delta K}$) and therefore was unable to
84 form covalent bonds with PG, did not synchronize the division of OM with the IM or PG
85 (**Fig. 1A8, 1B**). Similar to most Gram-negative bacteria, *M. xanthus* possesses a conserved
86 Tol-Pal system and several OmpA-like OMPs, albeit cryoEM and fluorescence imaging
87 demonstrated that their native expression fails to couple the OM to PG during division
88 (**Fig. 1A1 - 1A3**). However, similar to the exogenous Lpp, endogenous overexpression of
89 Pal successfully synchronized the invagination, constriction, and separation of OM with
90 both the IM and PG (**Fig. 1A6, 1A7, 1B**). Thus, reinforcing the OM-PG connection is
91 sufficient to synchronize their division.

92 This study demonstrates that while Gram-negative bacteria commonly coordinate
93 PG and OM synthesis [7,25], coupled constriction and fission of these two cell wall layers is

not universally conserved for cell division. OM division may occur autonomously through a solely physical mechanism, independent of PG-tethering.

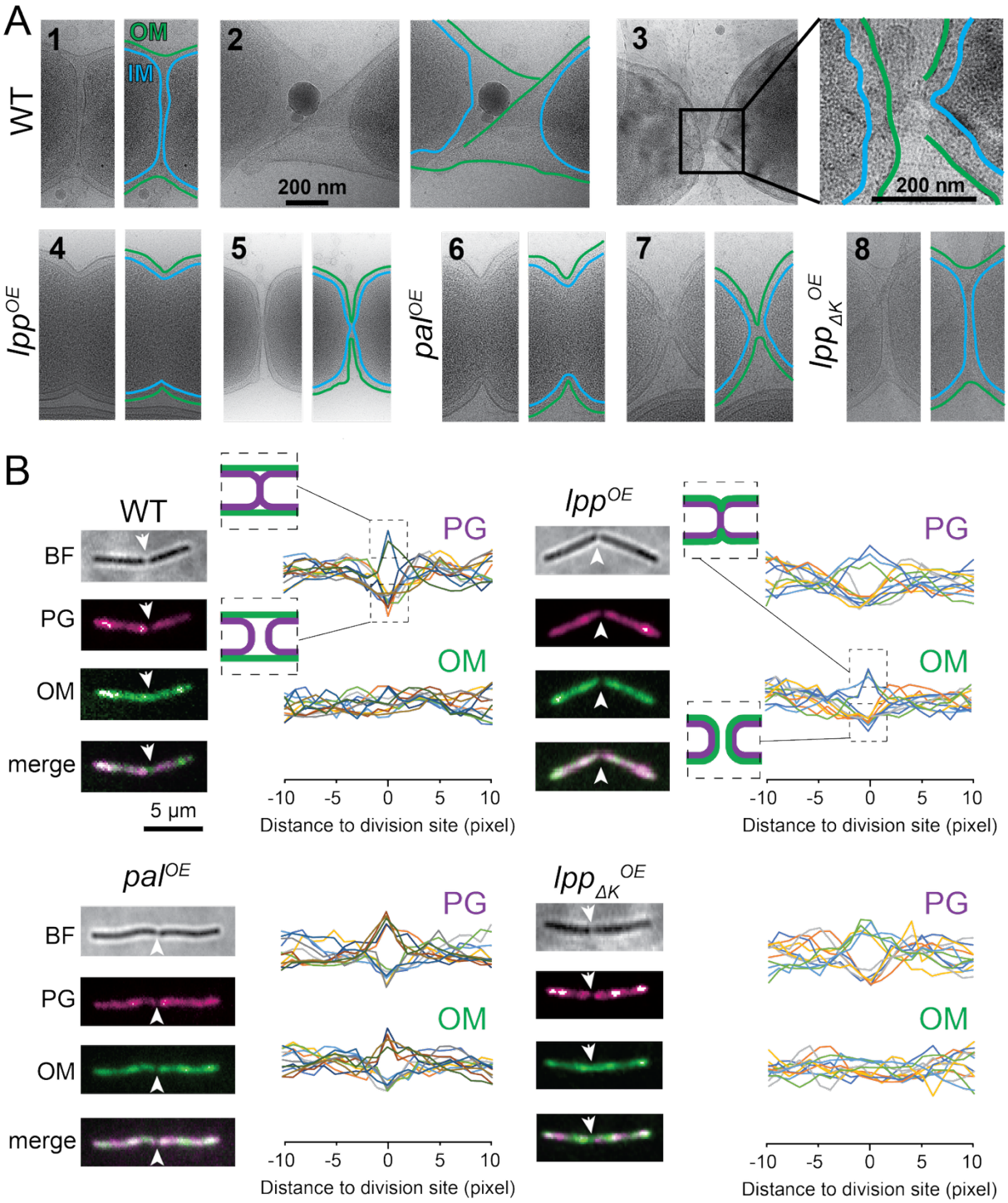

Fig. 1. Uncoupled division of PG and the OM in the Gram-negative bacterium *M. xanthus*. A) Cryo-EM images of the OMs and IMs at division sites in the wild-type (WT) cells (**1**, the OM remained connected after the division of IM; **2**, the stretched and twisted OM at a division site; **3**, OM fracture when the daughters cells separate), the cells exogenously overexpressing *E. coli* Lpp that attaches the OM to PG (lpp^{OE}, **4** and **5**), the ones overexpressing Pal endogenously (pal^{OE}, **6** and **7**), and the ones exogenously overexpressing a truncated *E. coli* Lpp that cannot attach the OM to PG ($lpp_{\Delta K}^{OE}$, **8**). **B)** Fluorescence images of the OM and PG in division cells. BF, bright field. White arrows point to the division sites. The fluorescence intensities of PG and OMs from 12 cells are shown for each strain. The identities of cells are distinguished by colors and the fluorescence intensity values of PG and OM were normalized using Z-score standardization.

111 **Materials and methods**

112 Vegetative *M. xanthus* cells were grown in liquid CYE medium (10 mM MOPS pH 7.6,

113 1% (w/v) Bacto™ casitone (BD Biosciences), 0.5% yeast extract and 8 mM $MgSO_4$) at

114 32 °C, in 125-ml flasks with vigorous shaking, or on CYE plates that contains 1.5% agar.

115 We used strain DZ2 as the wild-type *M. xanthus* strain [26]. Overexpression mutants were

116 constructed by electroporating DZ2 cells with 4 μg of plasmid DNA. The genes, driven

117 by a vanilate-inducible promoter, were inserted into the Mx4 phage attachment site as

118 merodiploids on the *M. xanthus* chromosome. Transformed cells were plated on CYE

119 plates supplemented with 10 mg/ml tetracycline and expression was induced by 100

120 μM sodium vanilate. The strains and plasmids used in this study are listed in **Table S1**.

121 **Table S1. Strains and plasmids used in this study**

Strain name	Description	Source
DZ2	The wild-type strain	[26]
BN380	DZ2 with P_{van}-*lpp*	This study
BN381	DZ2 with P_{van}-$lpp_{\Delta K}$	This study
BN382	DZ2 with P_{van}-*pal*	This study

Plasmid name	Description	Source
pMR3629	Plasmid for overexpressing genes as merodiploids using a vanilate-induced promoter, tet^R	[27]
pMR3629-lpp	P_{van}-*lpp* in pMR3629, tet^R	This study
pMR3629-$lpp_{\Delta K}$	P_{van}-$lpp_{\Delta K}$ in pMR3629, tet^R	This study
pMR3629-pal	P_{van}-*pal* in pMR3629, tet^R	This study

122 Bacterial strains were grown overnight in CYE media with appropriate antibiotics,

123 incubated with shaking at 32 °C and 250 rpm to an optical density of OD_{600} 0.6. Cells were

124 collected by centrifugation (3 min, 6,000 × g, 25 °C) and resuspended in CYE media to a
125 final OD_{600} 12. This cell suspension (3 µl) was applied to C Flat-1.2/1.3 200 mesh copper
126 grids (Electron Microscopy Sciences) that were glow discharged for 30 seconds at 15 mA.
127 Grids were plunge-frozen in liquid ethane with an FEI Vitrobot Mark IV (Thermo Fisher
128 Scientific) at 4 °C, 100% humidity with a waiting time of 30 s, two-side blotting time of
129 2.5 - 3 s, and blotting force of 0. All subsequent grid handling and transfers were
130 performed in liquid nitrogen. Grids were clipped onto cryo-FIB autogrids (Thermo Fisher
131 Scientific).

132 Images were acquired using a Thermo Fisher Scientific Titan Krios G4 transmission
133 electron microscope, equipped with a Gatan K3 direct electron detector and a Gatan
134 BioContinuum energy filter. Imaging was performed using a 15 eV slit width on the
135 energy filter to enhance image contrast. Micrographs were recorded in counted mode at
136 a nominal magnification of 33,000x, using a dose rate of 14.65 electrons/pixel/second over
137 a 2.6-second exposure, resulting in a total accumulated dose of 50 electrons/$Å^2$.

138 For fluorescence microscopy, cultures were grown in liquid CYE to OD_{600} ~1 and
139 supplemented with 10 µg/mL wheat germ agglutinin Alexa Fluor-488 conjugate and 75
140 µM TADA for one hour. Cells were spun down at 6,000x g for 3 min and the pellet washed
141 three times with CYE. 5 µl of cells were spotted on agar (1.5%) pads and imaged using a
142 Andor iXon Ultra 897 EMCCD camera (effective pixel size 160 nm) on an inverted Nikon

143 Eclipse-Ti™ microscope with a 100× 1.49 NA TIRF objective. Fluorescence of TADA and

144 Alexa Fluor 488-conjugated wheat germ agglutinin was excited by the 561-nm and 488-

145 nm lasers, respectively. Fluorescence intensities were quantified using the ImageJ suite

146 (https://imagej.net) and normalized by Z-score standardization using $Z = (\chi - \mu)/\sigma$, where

147 Z, χ, μ, and σ are the standard score, observed value, mean, and standard deviation,

148 respectively.

149 **Acknowledgments**

150 We thank Drs. Michael Van Nieuwenhze and Yen-Pang Hsu for providing TADA, Dr. Gaya
151 Yadav for the assistance on cryoEM imaging, and all the members in the Nan laboratory for
152 technical support and constructive discussions. This work was supported by the National
153 Institutes of Health grants GM129000 to B. N..

154

References

1 Henderson, J. C. *et al.* The Power of Asymmetry: Architecture and Assembly of the Gram-Negative Outer Membrane Lipid Bilayer. *Annu Rev Microbiol* **70**, 255-278 (2016). https://doi.org/10.1146/annurev-micro-102215-095308

2 Blair, J. M. A., Webber, M. A., Baylay, A. J., Ogbolu, D. O. & Piddock, L. J. V. Molecular mechanisms of antibiotic resistance. *Nature Reviews Microbiology* **13**, 42-51 (2015). https://doi.org/10.1038/nrmicro3380

3 Fivenson, E. M. *et al.* A role for the Gram-negative outer membrane in bacterial shape determination. *Proc Natl Acad Sci U S A* **120**, e2301987120 (2023). https://doi.org/10.1073/pnas.2301987120

4 Rojas, E. R. *et al.* The outer membrane is an essential load-bearing element in Gram-negative bacteria. *Nature* **559**, 617-621 (2018). https://doi.org/10.1038/s41586-018-0344-3

5 Cameron, T. A. & Margolin, W. Insights into the assembly and regulation of the bacterial divisome. *Nat Rev Microbiol* **22**, 33-45 (2024). https://doi.org/10.1038/s41579-023-00942-x

6 Mathelie-Guinlet, M., Asmar, A. T., Collet, J. F. & Dufrene, Y. F. Lipoprotein Lpp regulates the mechanical properties of the *E. coli* cell envelope. *Nature communications* **11**, 1789 (2020). https://doi.org/10.1038/s41467-020-15489-1

7 Mamou, G. *et al.* Peptidoglycan maturation controls outer membrane protein assembly. *Nature* **606**, 953-959 (2022). https://doi.org/10.1038/s41586-022-04834-7

8 Gray, A. N. *et al.* Coordination of peptidoglycan synthesis and outer membrane constriction during *Escherichia coli* cell division. *Elife* **4** (2015). https://doi.org/10.7554/eLife.07118

9 Typas, A. *et al.* Regulation of peptidoglycan synthesis by outer-membrane proteins. *Cell* **143**, 1097-1109 (2010). https://doi.org/10.1016/j.cell.2010.11.038

10 Paradis-Bleau, C. *et al.* Lipoprotein cofactors located in the outer membrane activate bacterial cell wall polymerases. *Cell* **143**, 1110-1120 (2010). https://doi.org/10.1016/j.cell.2010.11.037

11 Szczepaniak, J. *et al.* The lipoprotein Pal stabilises the bacterial outer membrane during constriction by a mobilisation-and-capture mechanism. *Nature communications* **11**, 1305 (2020). https://doi.org/10.1038/s41467-020-15083-5

12 Reusch, R. N. Insights into the structure and assembly of *Escherichia coli* outer membrane protein A. *FEBS J* **279**, 894-909 (2012). https://doi.org/10.1111/j.1742-4658.2012.08484.x

13 Navarro, P. P. *et al.* Cell wall synthesis and remodelling dynamics determine division site architecture and cell shape in *Escherichia coli*. *Nat Microbiol* **7**, 1621-1634 (2022). https://doi.org/10.1038/s41564-022-01210-z

14 Aramayo, R. & Nan, B. *De Novo* Assembly and Annotation of the Complete Genome Sequence of *Myxococcus xanthus* DZ2. *Microbiol Resour Announc*, e0107421 (2022). https://doi.org/10.1128/mra.01074-21

15 Topo, E. J., De Santiago, C. B., Cao, P., Wall, D. & Nan, B. Mechanism of bacterial outer membrane exchange revealed by quantitative microscopy. *bioRxiv*, 2025.2004.2025.650704 (2025). https://doi.org/10.1101/2025.04.25.650704

16 Remis, J. P. *et al.* Bacterial social networks: structure and composition of *Myxococcus xanthus* outer membrane vesicle chains. *Environ Microbiol* **16**, 598-610 (2014). https://doi.org/10.1111/1462-2920.12187

17 Subedi, K., Roy, P. C., Saiz, B., Basile, F. & Wall, D. Cell-cell transfer of adaptation traits benefits kin and actor in a cooperative microbe. *Proc Natl Acad Sci U S A* **121**, e2402559121 (2024). https://doi.org/10.1073/pnas.2402559121

18 Sheng, Q. *et al.* In situ visualization of Braun's lipoprotein on *E. coli* sacculi. *Sci Adv* **9**, eadd8659 (2023). https://doi.org/10.1126/sciadv.add8659

19 Hsu, Y. P. *et al.* Full color palette of fluorescent d-amino acids for in situ labeling of bacterial cell walls. *Chem Sci* **8**, 6313-6321 (2017). https://doi.org/10.1039/c7sc01800b

20 Dubois, L., Vettiger, A., Buss, J. A. & Bernhardt, T. G. Using fluorescently labeled wheat germ agglutinin to track lipopolysaccharide transport to the outer membrane in *Escherichia coli*. *mBio* **16**, e0395024 (2025). https://doi.org/10.1128/mbio.03950-24

21 Fu, G. *et al.* MotAB-like machinery drives the movement of MreB filaments during bacterial gliding motility. *Proc Natl Acad Sci U S A* **115**, 2484-2489 (2018). https://doi.org/10.1073/pnas.1716441115

22 Nan, B. *et al.* The polarity of myxobacterial gliding is regulated by direct interactions between the gliding motors and the Ras homolog MglA. *Proc Natl Acad Sci U S A* **112**, E186-193 (2015). https://doi.org/10.1073/pnas.1421073112

23 Nan, B. *et al.* Flagella stator homologs function as motors for myxobacterial gliding motility by moving in helical trajectories. *Proc Natl Acad Sci U S A* **110**, E1508-1513 (2013). https://doi.org/10.1073/pnas.1219982110

24 Tokunaga, M., Imamoto, N. & Sakata-Sogawa, K. Highly inclined thin illumination enables clear single-molecule imaging in cells. *Nat Methods* **5**, 159-161 (2008). https://doi.org/10.1038/nmeth1171

25 Hummels, K. R. *et al.* Coordination of bacterial cell wall and outer membrane biosynthesis. *Nature* **615**, 300-304 (2023). https://doi.org/10.1038/s41586-023-05750-0

26 Campos, J. M. & Zusman, D. R. Regulation of Development in *Myxococcus-xanthus* - Effect of 3' Doublebond 5'-Cyclic Amp, Adp, and Nutrition. *Proceedings of the National Academy of Sciences of the United States of America* **72**, 518-522 (1975). https://doi.org/DOI 10.1073/pnas.72.2.518

27 Iniesta, A. A., Garcia-Heras, F., Abellon-Ruiz, J., Gallego-Garcia, A. & Elias-Arnanz, M. Two systems for conditional gene expression in *Myxococcus xanthus* inducible by isopropyl-beta-D-thiogalactopyranoside or vanillate. *J Bacteriol* **194**, 5875-5885 (2012). https://doi.org/10.1128/JB.01110-12